

**Label-Free Analysis of Binding and Inhibition of SARS-CoV-19 Spike Proteins to ACE2
Receptor with ACE2-derived Peptides by Surface Plasmon Resonance**

Fatimah Abouhajar, Rohit Chaudhuri, Santino N. Valiulis, Daniel D. Stuart, Alexander S. Malinick, Min Xue, and Quan Cheng*

Department of Chemistry
University of California, Riverside, CA 92521

*Corresponding author: Quan Cheng

Tel: (951) 827-2702

Fax: (951) 827-4713

Email: quan.cheng@ucr.edu

ABSTRACT:

SARS-CoV-2 has been shown to enter and infect host cells via an interaction between spike protein (S glycoprotein), and angiotensin-converting enzyme 2 (ACE2). As such, it may be possible to suppress the infection of the virus via the blocking of this binding interaction, through the use of specific peptides that can mimic the human ACE 2 peptidase domain (PD) α 1 helix. Herein, we report the use of competitive assays along with surface plasmon resonance (SPR) to investigate the effect of peptide sequence and length on spike protein inhibition. The characterization of these binding interactions helps us understand the mechanisms behind peptide-based viral blockage and develops SPR methodologies to quickly screen disease inhibitors. This work not only helps further our understanding of the important biological interactions involved in viral inhibition but will also aid in future studies that focus on the development of therapeutics and drug options. Two peptides of different sequence lengths, [30-42] and [22-44], based on the α 1 helix of ACE2 PD were selected for this fundamental investigation. In addition to characterizing their inhibitory behavior, we also identified the critical amino acid residues of the RBD/ACE2-derived peptides by combining experimental results and molecular docking modeling. While both investigated peptides were found to effectively block the RBD residues known to bind to ACE2 PD, our investigation showed that the shorter peptide was able to reach a maximal inhibition at lower concentrations. These inhibition results matched with molecular docking models and indicated that peptide length and composition are key in the development of an effective peptide for inhibiting biophysical interactions. The work presented here emphasizes the importance of inhibition screening and modeling, as longer peptides are not always more effective.

INTRODUCTION:

The outbreak of coronavirus disease 2019 (COVID-19) caused by the severe acute respiratory syndrome coronavirus 2 (SARS-CoV-2) has infected over 600 million individuals and has resulted in the death of over 6.4 million people as of September 2022, according to the World Health Organization (WHO).¹ While a great deal of effort has gone into developing new ways to treat and prevent the onset of COVID-19,²⁻⁵ it is still affecting many people around the world, and it appears that it will continue to be present for the foreseeable future.⁶

At the molecular level, the infection of SARS-CoV-2 is driven by a crucial interaction between the viral spike protein and the human ACE2 protein,⁷ whose normal function is to catalyze the hydrolysis of the vasoconstrictor peptide angiotensin II.^{8,9} To gain a deeper understanding of the interaction observed between SARS-CoV-2 and ACE2 one must understand the structure of SARS-CoV-2. The overall structure of the virus consists of a 30 kD single-stranded RNA genome that is encapsulated by a lipid bilayer and three distinct structural proteins that are embedded within the lipid membrane: envelope (E), membrane (M), and spike (S).¹⁰ The spike protein is a large (1208 residue), heavily glycosylated polypeptide that forms homotrimers which are what gives the Coronavirus its "corona" structure in electron micrographs. Each monomer consists of two subunits (S1 and S2), where the key receptor-binding domain (RBD) corresponds to residues 319-541 and falls within the S1 subunit.¹¹ In a demonstration of the high-resolution capabilities of CryoEM technologies, the full-length structure of the spike protein was determined at 2.8 Å within months of the global onset of COVID-19 (PDB 6VXX, 6VYB).¹² One of the most valuable insights to arise from these full-length structures was the occurrence of an "open" and "closed" configuration of the RBD relative to the rest of the protein, where only the "open" configuration is able to efficiently bind hACE2.^{12,13} This receptor binding induces the dissociation of the S1 with ACE2, prompting the S2 to transition from a metastable pre-fusion to a more stable post-fusion state that is essential for membrane fusion.¹⁴⁻¹⁶ Therefore it appears that the binding to the ACE2 receptor is a critical initial step for SARS-CoV-2 to enter into target cells.¹⁷ It is important to note that other mechanisms of spike protein induced cellular damage have been proposed that do not rely on the ACE2 receptor of SARS-CoV-2.^{18,19}

Further information regarding the importance of the onset of COVID-19 and the structure of SARS-CoV-2 was obtained through X-ray crystallography. Most notably, the information related to spike protein RBD in complex with hACE2 (PDB-ID: 6M0J, 6LZG, and 6VW1), which

greatly aided in understanding the lethality of the virus.²⁰⁻²² Several ACE2 and s-protein residues were identified as part of the ACE2/s-protein interaction by inspection of a crystal structure of the complex. Using the published crystal structure of the ACE2/s-protein RBD complex, amino acids at the ACE2 motifs and the viral s-protein RBD in the interface core were defined. In the recognition of RBD, it was found that the protease domain (PD) of ACE2 mainly engages the α 1-helix (Ser19-Gln42).²² By deciphering which key amino acid residues are in contact at the interface between the two proteins, the development of disruptors specific for the SARS-CoV-2/ACE2 protein-protein interaction (PPI) can be pursued.^{23, 24} This is significant as small-molecule inhibitors are often considered to be less effective at disrupting extended protein binding interfaces,²⁵ whereas peptides offer a synthetically accessible solution to disrupt PPIs by binding at interface regions containing multiple contact "hot spots".²⁶

Peptides, in a similar fashion as COVID-19 monoclonal antibodies (mAbs), aim to abrogate the SARS-CoV-2/ACE2 interaction.^{27, 28} CoV mAbs primarily target the trimeric S glycoproteins, and the majority recognize epitopes within the RBD that binds the ACE2 receptor.²⁸⁻³⁰ However, RNA viruses accumulate mutations over time, which yields antibody resistance and requires the use of antibody cocktails to avoid mutational escape.³¹ Not surprisingly, there is clear evidence of the emergence of SARS-CoV-2 mutants for which antibodies against the original strain have no or diminished activity.³² On the other hand, proteins or rigid peptides with specific (multivalent) binding domains could facilitate the development of COVID-19 treatments or vaccines³³ that are potentially independent of further viral S-protein mutation. Overall, peptide and protein therapies show high specificity, minimal interference with biological processes, good tolerance to human organisms, and faster FDA approval times.³⁴ Though more research into the fundamental interactions between protein interactions where peptides act as blockers is clearly still needed.

Recent computational studies have attempted to show that small molecules and peptide-mimetic inhibitors can inhibit SARS-CoV-2 s-protein interactions.³⁵ One study³⁶ focused on 23 residues from the first N-terminal helix of ACE2. MD simulations and free energy calculations were utilized to show that the 23-residue peptide, as well as a mutated variant, bound to the SARS-CoV2 s-protein RBD with high affinity. Another study³⁷ utilized similar MD-based methods in an in-silico study, and they reported a putative minimum binding epitope from the ACE2 N-terminal helices. This smaller peptide motif had retained binding strength for the s-protein RBD. These two

computational studies where the authors report ACE2 mimetic peptide inhibitors of s-protein binding could form the basis for the design of potential peptide-based SARS-CoV-2 therapeutics. This is significant as human recombinant soluble ACE2 (hrsACE2) is currently being considered as a treatment for COVID-19.^{38, 39} However, ACE2 is involved in many key cellular processes, such as blood- pressure regulation and other cardiovascular functions.⁴⁰ Therefore, hrsACE2 treatment could lead to dysregulation of those vital processes and subsequently cause deleterious side effects for treated patients. To avoid any interference of the ACE2 homeostasis, we wanted to test if and how small ACE2-derived peptides can also interfere with SARS-CoV-2 binding, by blocking binding sites on the S glycoprotein.

To this end, we synthesized and tested short ACE2-derived peptides targeting the viral S glycoprotein as potent binding inhibitor peptides and observed a significant reduction in the binding properties. We accomplished this by utilizing the label-free approach surface plasmon resonance, which provides highly sensitive detection capabilities. The first peptide (Glu22-Ser44) was selected to mimic the regions of ACE2 that interact with the S1 subunit as determined by the previously discussed crystal structure.²² The second one is a truncated version of the first peptide (D30-Q42). Next, we performed molecular docking using the PatchDock program aimed at gaining an in-depth understanding of the interaction between the SARS-CoV2 RBD and the ACE2-derived peptides. By gaining a deeper understanding of the interactions between peptides and viruses, such as ACE2 peptides' ability to inhibit SARS-CoV-2 binding, our findings have the potential to open up new avenues of research related to ways to treat and investigate viral diseases such as COVID-19. This is of great interest as peptides are generally considered to be highly selective, effective, and safe, making them ideal for future therapeutic uses.⁴¹

EXPERIMENTAL:

Materials:

Recombinant SARS-CoV-2 spike protein, S1 subunit (Val16-Gln690) was purchased from RayBiotech. Human ACE2, His tag (E.coli) was obtained from MP Biomedicals, LLC. 11-mercaptopundecanoic acid (MUA). O-(2-Aminoethyl)-methylpoly-ethylene glycol (PEGamine), N-Hydroxysuccinimide (NHS), and 1-(3-dimethylaminopropyl)-3-ethylcarbodiimide hydrochloride (EDC) were purchased from Sigma-Aldrich (St. Louis, MO). All protein solutions were prepared in 20 mM phosphate buffered saline (containing 150 mM NaCl, pH 7.4). Rink amide

MBHA resin was obtained from Aapptec (Louisville, KY). Fmoc-protected amino acids were obtained from Anaspec (Fremont, CA). Piperidine was purchased from Alfa Aesar (Ward Hill, MA). 2-(1H-benzotriazol-1-yl)-1,1,3,3-tetramethyluronium hexafluorophosphate (HBTU, 99.6%) and diisopropylethylamine (DIEA, 99.5%) were purchased from Chem-Impex (Wood Dale, IL) and ACROS (Germany) respectively. Triisopropylsilane (TIPS) was obtained from TCI (Portland, OR). α -cyano-4-hydroxycinnamic acid (CHCA) was purchased from Sigma Aldrich (St. Louis, MO). Crystal structure of SARS-CoV-2 spike receptor-binding domain bound with ACE2 PD at 2.45 \AA resolution with PDB ID: 6M0J was retrieved from RCSB PDB database (<https://www.rcsb.org/>).

Solid-phase peptide synthesis (SPPS) of linear peptides

CSBio CS336S peptide synthesizer (Menlo Park, CA) was used to synthesize the linear peptide sequences. 500 mg of Rink Amide resin with a loading capacity of 0.678 mmol/g was used for each synthesis. Fmoc-protected L-amino acids (1 mmol each), DIEA (0.8 M in DMF), HATU (0.4 M in DMF) were used for each coupling step, and 20% piperidine/DMF was used for Fmoc deprotection. At the end of synthesis, the resin was treated with a solution of TFA, tri-isopropyl silane, and water (95:2.5:2.5 by volume) to cleave the peptide from the resin. The cleavage solution was mixed with cold diethyl ether to obtain the crude peptide as precipitates.

Purification of the synthesized peptides

The crude peptide was purified on a Thermo Ultimate 3000BX HPLC, equipped with a preparative column (Kinetex 5 μm EVO, 250 \AA \sim 21.2 mm²). A gradient of 0–100% acetonitrile (with 0.1% TFA) in water (with 0.1% TFA) was used. The identity of each fraction was confirmed by MALDI-TOF on a SCIEX 5800 mass spectrometer. Fractions containing the product were pooled and lyophilized to obtain the pure peptide.

SPR analysis of ACE2-derived peptide inhibition of SARS-CoV-19 spike protein binding:

A dual channel SPR spectrometer NanoSPR-321 (NanoSPR, Addison, IL) with a GaAs semiconductor laser light source ($\lambda = 670$ nm) was used for all SPR measurements. The device comes with a high-refractive index prism ($n = 1.61$) and 30 μL flow cell. SPR gold chips were fabricated with a 2 nm thick chromium adhesion layer, followed by deposition of a 46 nm thick gold layer via e-beam evaporation onto cleaned BK-7 glass slides based on previously published procedures.⁴²

Surface interactions were monitored using angular scanning mode which tracks the angle of minimum reflectivity. The gold substrate was incubated in 1 mM MUA ethanol solution for 18 h to form a self-assembled monolayer with carboxyl functional groups on the surface. After extensive rinsing with ethanol and DI water, the chip was dried under an air stream. The gold substrate was then clamped to a flow cell on a prism. To activate the carboxyl acid group, EDC (0.4 M)/NHS (0.1 M) solution was injected into the flow cell and incubated for 30 min. After 10 min of rinsing, 0.5 μ g/ml of spike protein in PBS at a pH of 7.4 was injected and incubated for 1 hr to allow the formation of covalent amide linkages. Followed by a 10 min rinse to eliminate any residual spike protein in the solution. Passivation of the unused activated carboxyl groups was performed by incubation with 10 mg/ml PEG amine solution for 1 hr. Then the inhibition assay was performed. All protein binding and inhibition studies were performed under identical buffer conditions with pH 7.4 PBS.

Preparation of both receptor and peptide molecules

The human coronavirus spike protein structures and ACE2 structure were downloaded from the RCSB protein data bank. ACE2 structures were modified manually to produce the derived peptide structures. Depending on the peptide needed, the appropriate section of ACE2 was isolated so as to run future docking simulations. In addition, the binding domain on the spike protein was separated from the rest of the structure to specify the interactions between the binding domain and ACE2-derived peptides. The structures of the peptides and spike protein binding domain were verified after editing using PyMOL.

Molecular Docking

The MD between human coronavirus spike protein and each peptide under study were performed using PatchDock web server. PatchDock is developed as a geometry-based MD algorithm. It calculates the docking transformation between two molecules to get the best molecular interface complementarity. Which ascertains the peptide posture in relation to the receptor with maximal interface area coverage and minimal steric hindrance.⁴³ Each ACE2-derived peptide was docked with SARS-CoV-2 RBD by uploading the molecules to the Patchdock server, an automatic server for molecular docking. Clustering RMSD was chosen as 4.0 \AA . PyMOL was used to analyze the docking results of RBD/ACE2 derived peptide interaction by identifying the original binding residue between the RBD/ACE2 PD complex.

RESULT AND DISCUSSION:

The N-terminal region of the ACE2 PD is critical for binding to the SARS-CoV-2 spike protein

In order to investigate the best attributes to explore when designing a small peptide-based inhibitor that can block the interaction of SARS-CoV-2 spike protein with the ACE2 receptor, we investigated existing structures of known amino acid interactions necessary for binding of SARS-CoV-2 to ACE2 (Table. 1). This includes the crystal structure of the ACE2 PD/RBD complex (PDB ID: 6m0j, 6vw1, and 6LZG) in addition to the full length of the ACE2 with SARS-CoV-2 complex (PDB ID: 6M17). Comparisons of the ACE2 interacting residues with SARS-CoV-2 spike protein according to the previous analysis of ACE2/RBD crystal structures^{20-22, 24} are shown in Table 2 and Table 3. It is clear from the table that the α 1 helix (S19-S44) of ACE2 provides the most contact with the SARS-CoV-2 RBD, as well as a small area on the α 2 helix, the short loop between α 10/ α 11, and the linker between β 3/ β 4. Therefore, selection of the peptide-based inhibitor was chosen based upon this insight and recent work published by Zhang et al.⁴⁴ Where they suggested that the 23-mer peptide mimics the α -1 helix as a potential drug for SARS-CoV2 and its affinity to bind to the viral RBD was also demonstrated. The energies involved in the binding of the isolated peptide to the viral RBD was expected to be close to that of the RBD-ACE2 complex.

Consequently, the [22-44] peptide (Glu22-Ser44, wheat ribbon in fig 1B) has been synthesized to mimic the α -1 helix and tested for its ability to interfere with SARS-CoV-2-spike protein/ACE2 binding. In addition, a smaller peptide was obtained by removing the first 8 and last 2 histidine residues of the original [22-44] peptide. This 13-residue peptide was also synthesized and tested as an inhibitor of the ACE2/S1 complex. This small peptide (Asp30-Gln42, pink ribbon in fig 2B) contains most of the key contact with the RBD and represents the central and C-terminal of the isolated α -1 helix of ACE2. Here we aim to investigate the effect of changing the peptide length and residue coverage on the blocking efficiency of the Spike protein.

Evaluation of Blocking Efficiency Using Competition Surface Plasmon Resonance (SPR)

SPR is a well-established technique that has been utilized to investigate various biophysical interactions, especially those targeting proteins.⁴⁵⁻⁴⁸ However, direct analysis of the interaction between small molecules, such as small peptides, and a protein by SPR has always been a difficulty, largely due to the low signal change caused from small molecule interactions.⁴⁹ We, therefore, utilized a competition assay to evaluate the binding of the peptide to the SARS-CoV-2-

spike protein using SPR spectroscopy. Figure 1 provides a schematic of the competition assay. 50 $\mu\text{g/ml}$ of SARS-CoV-2-spike protein was immobilized on a self-assembled monolayer with a carboxyl functional group on the gold chip surface. An SPR competitive assay was then utilized to assess the ability of the ACE2-derived peptides to block the interaction between human ACE2 and SARS-CoV-2 spike protein. Peptides with different concentrations were mixed with 30 $\mu\text{g/ml}$ of human ACE2 protein and injected onto the chip coated with SARS-CoV-2-spike protein. Free human ACE2 solution (30 $\mu\text{g/ml}$) was injected as a control. To confirm the specificity of ACE2/spike protein interaction, we also conducted an additional independent control experiment using -COOH terminated alkanethiol surface without the spike protein.

Figure 2A depicts the SPR binding response of ACE2/spike protein with no inhibition, ACE2/spike protein in the presence of 0.1 $\mu\text{g/ml}$ of each peptide, and the independent control which represents ACE2 binding to S1 surface free. The SPR binding shift observed during the independent control experiment is significantly lower, thereby confirming the specificity of the ACE2/spike protein complex under our experimental conditions. Figure 2B and 2D demonstrate that increasing the concentration of both peptides decreases the binding signal of the ACE2 protein to SARS-CoV-2-spike protein coated on the chip, indicating a concentration-dependent inhibition of the peptides to the spike protein.

To visually compare the binding signal between the S1 subunit and ACE2 in the absence of the peptide (0 $\mu\text{g/ml}$) with the signal after adding the peptides at different concentrations (0.1, 1, 10, and 100 $\mu\text{g/ml}$), we plotted the SPR angle response versus the peptide's concentration (fig 2C). We found that the ACE2/spike protein binding caused an angle shift of 0.147 ± 0.009 degrees. The [22-44] peptide showed a maximum SPR angle inhibition of the ACE2/S1 complex formation with a measured reduction in SPR signal of 0.047 ± 0.009 degrees. It is of note that the small peptide, [30-42], shows a similar maximum inhibition potential at (0.049 ± 0.027 degrees). This result suggests that both peptides are able to disrupt the ACE2/spike protein interactions. In addition, this could indicate that the central and C-terminal region of the isolated α -1 helix of ACE2 is the essential motif important for disrupting the ACE2/S1 interaction since both peptides show similar max inhibition effects.

Based on the crystal structure of SARS-CoV-2 spike protein and ACE2 receptor (PDB ID: 6m0j) solved by Lan et al.²² the polar residues [24, 30, 35, 37, 38, 41, 42] of ACE2 helix-1 are the key interfacial interactions and are able to form a network of hydrogen bonds with the SARS-CoV-

2 spike protein. Accordingly, we can exhibit 6 critical amino acids that are part of both peptides under our study (at the central and C-terminal region). While [22-44] peptide has only one extra critical residue at the N-terminal region of the peptide. Moreover, it has been highlighted in the modeling study of RBD/ACE2 that the residues 37, 38, 41, and 42 are the key interfacial interactions between ACE2 and the RBD/spike protein.²⁰ Taken together, these structural insights and MD study lend support to our result of [22-44] and [30-42] as peptide disruptors of the ACE2/S1 interaction and that the central and C-terminal of the isolated α -1 helix of ACE2 contain more critical residue compared to N-terminal of the isolated α 1 helix of ACE2 PD.

When examining Figures 2 B, C, and D in more detail, it was found that the [30-42] peptide reached higher blocking efficiency and achieved saturation of the spike protein at lower concentrations compared to the [22-44] peptide. In the case of the [30-42] peptide, a 0.057 ± 0.02 degree reduction of SPR signal was observed at 1 μ g/ml. At the same concentration, the [22-44] peptide shows only 0.098 ± 0.007 degree reduction of the SPR signal. In addition, at 10 μ g/ml the [30-42] peptide showed a maximum neutralization to the spike protein. On the other hand, the [22-44] peptide indicates similar maximum neutralization, however, at a higher concentration (100 μ g/ml). This is possibly attributed to the presence of two consecutive serine residues in the [22-44] peptide, which could affect the peptides flexibility. As it has been shown that the presence of two consecutive serine residues affects the [37-45] peptide binding affinity to spike protein.⁵⁰

Next, we determined the half-maximal inhibitory concentration (IC50) of each peptide. Figures 3A and 3B show that the [22-44] and [30-42] peptides blocked the SARS-CoV-2 spike protein/ACE2 interaction with an IC50 value of 2.00 and 0.65 μ g/ml, respectively. This implies that the two peptides exhibit a strong affinity to the spike protein, although the [22-44] peptide has extra amino acid residues. This is of interest as Yang et al.⁵¹ suggested that the additional amino acids do not influence the overall affinity of the peptide for SARS-CoV-2 S1 subunit. Their experimental study used two peptides [22-44] and [22-57], which showed similar inhibition potential of the ACE2/spike complex. This was also supported by their MD simulation, which showed the [22-57] peptide established fewer hydrogen bonds when compared to that of the shorter one, [22-44] peptide. Moreover, it was reported that the residues 21-43 of the same human ACE2 α 1-helix (similar to [22-44] peptide under study) could strongly bind to SARS-CoV-2 RBD with micromolar affinity ($K_D = 1.3\mu\text{M}$)¹³ that is comparable to the full-length ACE2 binding to RBD²³.

Molecular Docking of ACE2-derived peptide/RBD interaction

In order to evaluate and compare the two peptides as inhibitors of the ACE2/S1 complex, we combined molecular docking with the experimental study. Molecular docking was performed through the PatchDock server to study the binding efficiency and to identify the important amino acid residues that contribute to the binding of the RBD/ACE2-derived peptide complex.

We evaluated the binding structure of the 23 and 13-amino acid chain, [22-44] and [30-42] peptides, respectively, alone and without the remainder of the ACE2 PD domain to the SARS-CoV-2 spike protein. To perform a non-biased analysis, we performed a blind docking run whereby we did not specify the binding site during the docking simulations. The obtained results were analyzed by comparing the docked conformations of each peptide within the SARS-CoV-2 spike protein. A contact was defined to exist between a peptide residue and the RBD if any atom of the RBD fell within 3 A° of any atom belonging to the peptide residue.

At the same time, we retrieved the crystal structure of the SARS-CoV-2 spike protein with the ACE2 PD domain (PDB ID: 6M0J) and explored it as the basis of the current study. The interface residues between the SARS-CoV-2 spike protein and the ACE2 PD domain were visualized and interpreted using Pymol software. After a detailed analysis of interface residues, the α 1 helix, which is cradled in a concave groove formed by β 5 and β 6 sheets of the RBD, provides the majority of the interaction between the ACE2/RBD interface (fig.4). Specifically, 8 residues (N487, K417, Q493, Y505, Y449, T500, N501, G446) in RBD provide contact via hydrogen bond with ACE2 (fig. 4A and 4B).

Figure. 3C shows the structural alignment of both the docked result of the peptide/RBD complex and the α 1 helix/RBD complex, which were constructed from the ACE2/RBD complex (PDB ID 6m0j). It is clear from the docking result that the [30-42] peptide binds to the concave groove of the RBD that the original ACE2 PD domain also binds. The [22-44] peptide laid on the RBD groove as well; however, only the central and the C-terminus of the peptide showed binding. This result aligns very well with the experimental results that the two peptides independently have the potential to inhibit the interaction of the SARS-CoV-2 spike protein and ACE2 complex but the shorter peptide results in more efficient inhibition.

By analyzing the docking results, the critical interacting amino acids of RBD/ACE2 were identified. Examination of Figures 5A and 5B presents that the RBD residues (449, 496, 493, 494, 500, 502, 505) were blocked by the [30-42] peptide. Similarly, the 35, 37, 38, and 41 residues of

the [22-44] peptide have the ability to occupy the RBD residues (449, 498, 496, 494, 493, 502) by making 6 Hydrogen bonds within 3°A. It is clear that most of the RBD-interacting amino acidic residues, as defined by PatchDock analysis, were within the prominent binding sites. This finding was consistent with the crystal structure of the ACE2/RBD complex (fig. 4A and 4B). The docking position of the two peptides in the RBD pocket ensured a high possibility of blocking the interaction with the ACE2 receptor, which is in alignment with our experimental results (fig. 2).

In addition, an inspection of the binding between each peptide and the RBD shows that fewer hydrogen bonds formed between the RBD/ peptide [22-44] complex compared with the RBD/peptide [30-42] complex, which makes 8 hydrogen bonds. This result is in line with our experimental results in which the [30-42] peptide shows higher inhibition of the ACE2/spike protein interaction for 0.1 to 1 µg/ml concentrations (fig. 2C) compared to the [22-44] peptide. It may be recalled that this result is in synergy with another study which suggests that the addition of extra amino acids does not necessarily increase the hydrogen bond or the binding efficiency of the peptide toward the spike protein.⁵¹ With this data it indicates that 7 residues blocked by the smaller peptide are crucial targets for blocking the ACE2/RBD binding interaction.

CONCLUSION:

Here we reported the fundamental investigation of two peptides' abilities to inhibit the ACE/SARS-CoV-2 interaction. The two inhibitors of different sequence lengths based on the α 1 helix of ACE2 PD showed similar blocking efficiency, with the shorter peptide reaching maximal blocking efficiency at a lower concentration. This demonstrates the feasibility of targeting ACE2/spike protein interaction interface with peptide-based inhibitors to inhibit virus infection. We observed a progressive reduction of the SPR binding signal as a function of the concentration confirming that specific inhibition was achieved. The [30-42] peptide, which is a truncated version of the longer peptide, highlights the importance of the amino acid residues at the central and C-terminus of the isolated α 1 helix of ACE2 for interaction with the spike protein. Moreover, we identified the critical residues of the RBD/ACE2 derived peptide interface using molecular docking, PatchDock. Analyzing the docking results revealed that the peptide inhibitors block most of the RBD residues that bind with ACE2, as predicted by analyzing the crystal structure of the ACE2/RBD complex. The results of our molecular docking and experimental inhibition assay were in alignment, indicating that small inhibitory peptides can effectively be used to block interactions

between ACE/SARS-CoV-2 spike protein complex. However, substantial work will be necessary to ensure effectiveness of an inhibitory peptide in vivo such as introduction of D-amino acids at N- and C- terminal regions to reduce proteolytic degradation.⁵² This small peptide inhibition assay with SPR demonstrates its potential as a platform for screening potential small molecule and peptide inhibitors to aid in the future investigation of drug discovery and development focused on peptides. The presented information and approach can be used to gain a deeper understanding of the RBD/ACE2 binding interaction, as well as aid in the development of an anti-SARS-CoV-2 treatment of the viral infection without the adverse side effects that exist for many other small molecules or recombinant protein therapeutic avenues.

Acknowledgements

QC would like to acknowledge the financial support from NSF (CHE-2109042). MX would like to acknowledge the financial support from NIH (R35 GM138214).

ORCID:

Quan Cheng: 0000-0003-0934-358X

Min Xue: 0000-0002-8136-6551

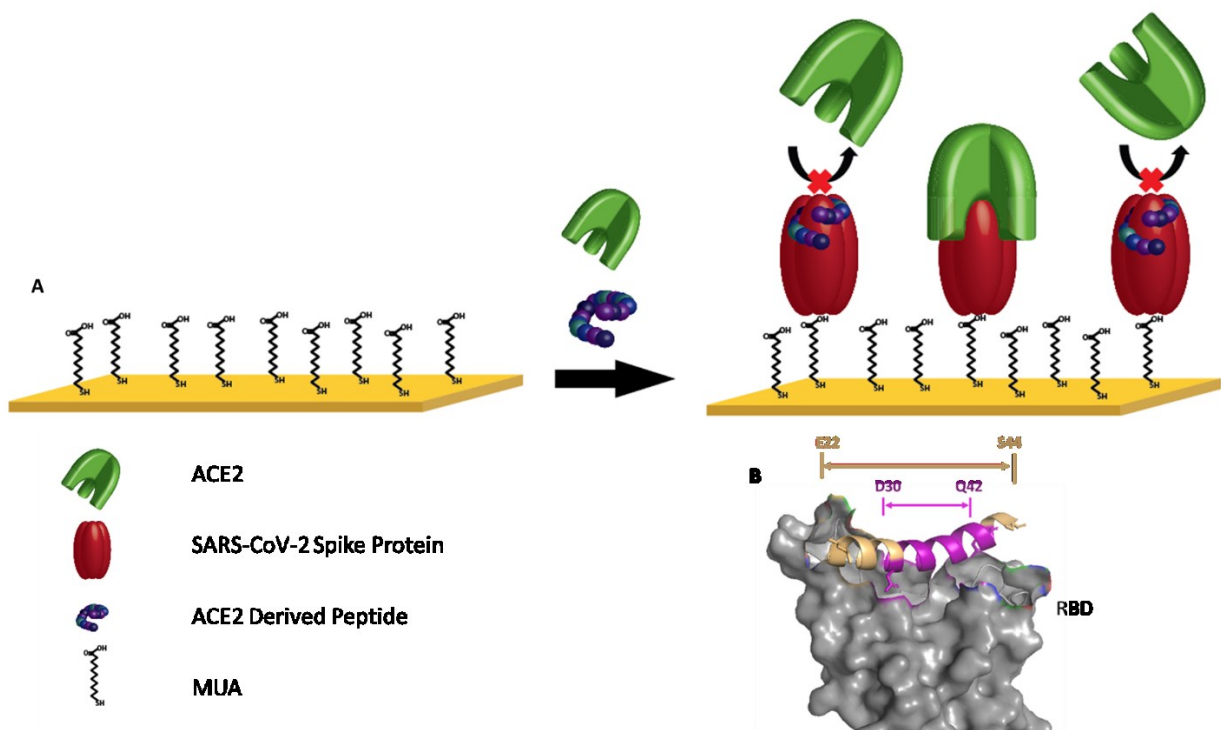


Figure 1. (A) Schematic of the competitive assay. (B) Relative location of [30-42] peptide (purple) and [22-44] peptide (tan) corresponding to PDB ID: 6m0j

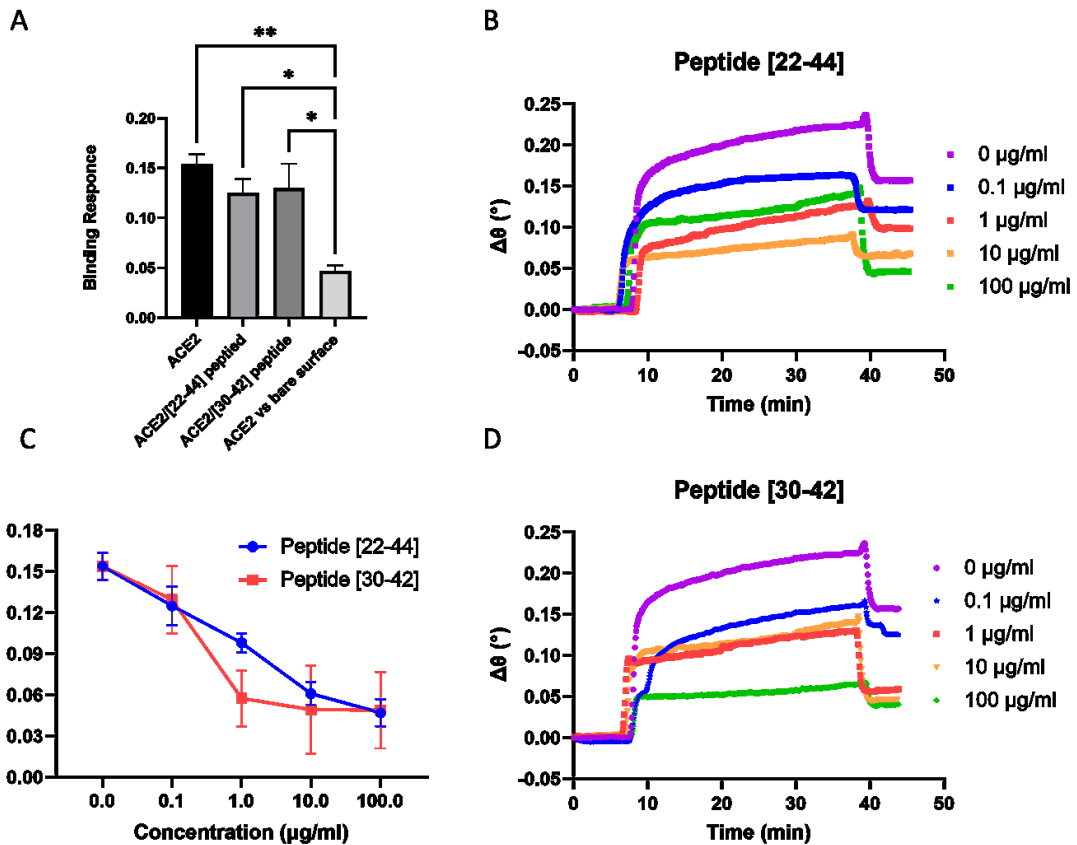


Figure 2. Evaluation of blocking efficiency of the ACE2-derived peptides to the S-protein using competitive SPR. A) Specific binding measured for the S-protein on the surface with ACE2. B) SPR sensorgrams with [22-44] peptide. C) The change of SPR binding signal as a function of peptide concentration. D) SPR sensorgrams with [30-42] peptide.

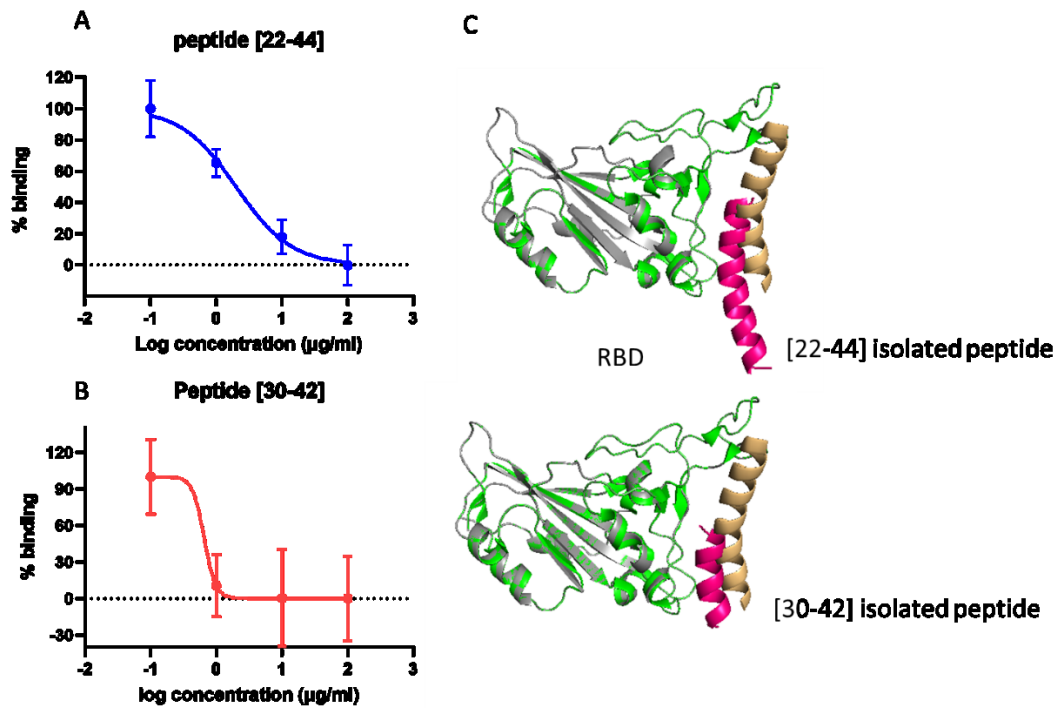
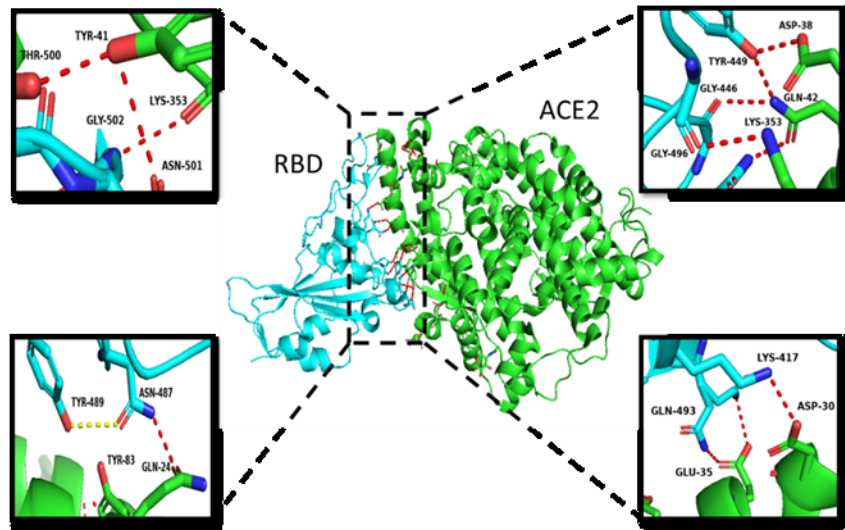


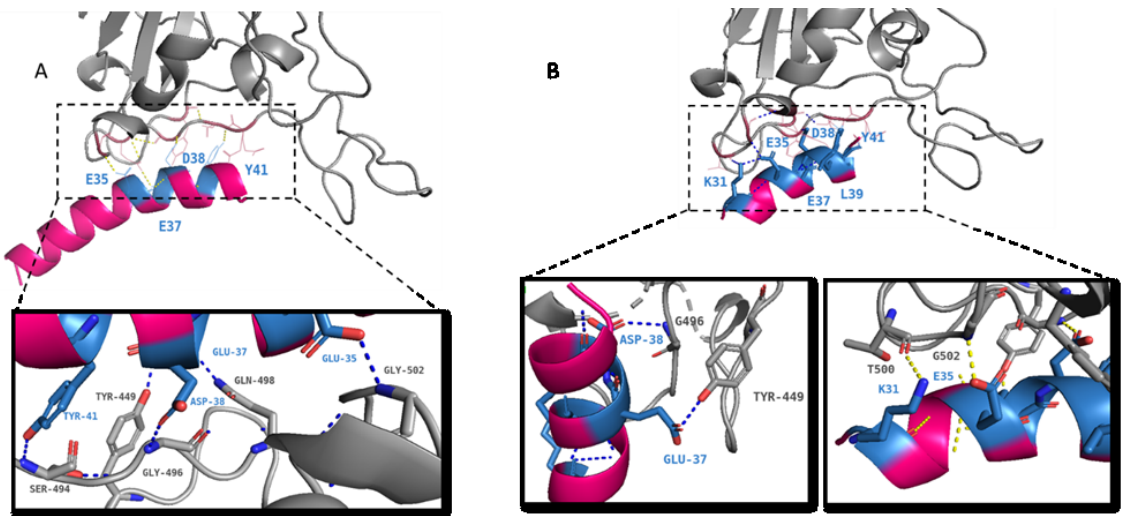
Figure 3. A) and B) Dose-dependent blocking of the S-protein with [22-44] and [30-42] peptides. C) structural alignment of both the docked result of the peptide/RBD complex and the α 1 helix/RBD complex, constructed from the ACE2/RBD complex (PDB ID 6M0J).



Interaction residues within 3A°

SARS-CoV-2 Spike RBD	Human ACE2
K417, G446, Y449, N487, Y489, Q493, T500, N501, and N502	Q24, D30, E35, E37, D38, Y41, Q42, Y83, K353, and R393

Figure 4. An illustration of the interacting interface of the SARS-CoV-2 receptor-binding domain (RBD) (cyan) and hACE2 (green) from PDB-ID: 6M0J. The key interacting residues are shown in close-up as insets. The table shows the interacting residues within a 3A° region analyzed using the PyMOL tool.



Interaction residues within 3A°		Interaction residues within 3A°	
SARS-CoV-2 Spike RBD	[22-44] peptide	SARS-CoV-2 Spike RBD	[30-42] peptide
Y449, Q493, S494, G496, Q498, and N502	E37, D38, Y41, Y41, and Q42	Y449, Y453, Q493, S494, T500, N502, and Y505	K31, E35, E37, D38, L39, Y41, and Q42

Figure 5. Interaction of the A) [22-44] peptide B) [30-42] peptide (pink) with the SARS-CoV-2 receptor-binding domain (RBD) (gray). Molecular docking complex obtained with PachDock. The key interacting residues are shown in close-up as insets. The table shows the interacting residues within a 3A° region analyzed using the PyMOL tool.

REFERENCES

1. WHO COVID-19 Dashboard. Geneva: World Health Organization 2020: Available online: <https://covid19.who.int/> Sept. 9th 2022.
2. Mahmud, N.; Anik, M. I.; Hossain, M. K.; Khan, M. I.; Uddin, S.; Ashrafuzzaman, M.; Rahaman, M. M., Advances in Nanomaterial-Based Platforms to Combat COVID-19: Diagnostics, Preventions, Therapeutics, and Vaccine Developments. *ACS Applied Bio Materials* **2022**, 5, 6, 2431–2460.
3. Karmacharya, M.; Kumar, S.; Gulenko, O.; Cho, Y.-K., Advances in facemasks during the COVID-19 pandemic era. *ACS Applied Bio Materials* **2021**, 4 (5), 3891-3908.
4. Yadav, S.; Sadique, M. A.; Ranjan, P.; Kumar, N.; Singhal, A.; Srivastava, A. K.; Khan, R., SERS Based Lateral Flow Immunoassay for Point-of-Care Detection of SARS-CoV-2 in Clinical Samples. *ACS Appl Bio Mater* **2021**, 4 (4), 2974-2995.
5. Pramanik, A.; Mayer, J.; Sinha, S. S.; Sharma, P. C.; Patibandla, S.; Gao, Y.; Corby, L. R.; Bates, J. T.; Bierdeman, M. A.; Tandon, R.; Seshadri, R.; Ray, P. C., Human ACE2 Peptide-Attached Plasmonic-Magnetic Heterostructure for Magnetic Separation, Surface Enhanced Raman Spectroscopy Identification, and Inhibition of Different Variants of SARS-CoV-2 Infections. *ACS Appl Bio Mater* **2022**, 5, 9, 4454–4464.
6. Parihar, A.; Ranjan, P.; Sanghi, S. K.; Srivastava, A. K.; Khan, R., Point-of-care biosensor-based diagnosis of COVID-19 holds promise to combat current and future pandemics. *ACS applied bio materials* **2020**, 3 (11), 7326-7343.
7. Kim, J.; Jeong, S.; Sarawut, S.; Kim, H.; Son, S. U.; Lee, S.; Rabbani, G.; Kwon, H.; Lim, E.-K.; Ahn, S. N. J. L. o. a. C., An immunosensor based on a high performance dual-gate oxide semiconductor thin-film transistor for rapid detection of SARS-CoV-2. **2022**, 22 (5), 899-907.
8. Li, W. H.; Moore, M. J.; Vasilieva, N.; Sui, J. H.; Wong, S. K.; Berne, M. A.; Somasundaran, M.; Sullivan, J. L.; Luzuriaga, K.; Greenough, T. C.; Choe, H.; Farzan, M., Angiotensin-converting enzyme 2 is a functional receptor for the SARS coronavirus. *Nature* **2003**, 426 (6965), 450-454.
9. Li, W.; Zhang, C.; Sui, J.; Kuhn, J. H.; Moore, M. J.; Luo, S.; Wong, S. K.; Huang, I. C.; Xu, K.; Vasilieva, N.; Murakami, A.; He, Y.; Marasco, W. A.; Guan, Y.; Choe, H.; Farzan, M., Receptor and viral determinants of SARS-coronavirus adaptation to human ACE2. *EMBO J* **2005**, 24 (8), 1634-43.
10. Chen, N.; Zhou, M.; Dong, X.; Qu, J.; Gong, F.; Han, Y.; Qiu, Y.; Wang, J.; Liu, Y.; Wei, Y.; Xia, J. a.; Yu, T.; Zhang, X.; Zhang, L., Epidemiological and clinical characteristics of 99 cases of 2019 novel coronavirus pneumonia in Wuhan, China: a descriptive study. *The Lancet* **2020**, 395 (10223), 507-513.
11. Ke, Z.; Oton, J.; Qu, K.; Cortese, M.; Zila, V.; McKeane, L.; Nakane, T.; Zivanov, J.; Neufeldt, C. J.; Cerikan, B.; Lu, J. M.; Peukes, J.; Xiong, X.; Krausslich, H. G.; Scheres, S. H. W.; Bartenschlager, R.; Briggs, J. A. G., Structures and distributions of SARS-CoV-2 spike proteins on intact virions. *Nature* **2020**, 588 (7838), 498-502.
12. Walls, A. C.; Park, Y. J.; Tortorici, M. A.; Wall, A.; McGuire, A. T.; Veesler, D., Structure, Function, and Antigenicity of the SARS-CoV-2 Spike Glycoprotein. *Cell* **2020**, 181 (2), 281-292 e6.
13. Xiong, X.; Qu, K.; Ciazznska, K. A.; Hosmillo, M.; Carter, A. P.; Ebrahimi, S.; Ke, Z.; Scheres, S. H. W.; Bergamaschi, L.; Grice, G. L.; Zhang, Y.; Collaboration, C.-N. C.-B.; Nathan, J. A.; Baker, S.; James, L. C.; Baxendale, H. E.; Goodfellow, I.; Doffinger, R.; Briggs, J. A. G., A thermostable, closed SARS-CoV-2 spike protein trimer. *Nat Struct Mol Biol* **2020**, 27 (10), 934-941.
14. Gui, M.; Song, W.; Zhou, H.; Xu, J.; Chen, S.; Xiang, Y.; Wang, X., Cryo-electron microscopy structures of the SARS-CoV spike glycoprotein reveal a prerequisite conformational state for receptor binding. *Cell Res* **2017**, 27 (1), 119-129.
15. Song, W.; Gui, M.; Wang, X.; Xiang, Y., Cryo-EM structure of the SARS coronavirus spike glycoprotein in complex with its host cell receptor ACE2. *PLoS Pathog* **2018**, 14 (8), e1007236.

16. Kirchdoerfer, R. N.; Wang, N.; Pallesen, J.; Wrapp, D.; Turner, H. L.; Cottrell, C. A.; Corbett, K. S.; Graham, B. S.; McLellan, J. S.; Ward, A. B., Stabilized coronavirus spikes are resistant to conformational changes induced by receptor recognition or proteolysis. *Sci Rep* **2018**, *8* (1), 15701.
17. Zamzami, M. A.; Rabbani, G.; Ahmad, A.; Basalah, A. A.; Al-Sabban, W. H.; Ahn, S. N.; Choudhry, H., Carbon nanotube field-effect transistor (CNT-FET)-based biosensor for rapid detection of SARS-CoV-2 (COVID-19) surface spike protein S1. *Bioelectrochemistry* **2022**, *143*, 107982.
18. Asandei, A.; Mereuta, L.; Schiopu, I.; Park, J.; Seo, C. H.; Park, Y.; Luchian, T., Non-receptor-mediated lipid membrane permeabilization by the SARS-CoV-2 spike protein S1 subunit. *J ACS Applied Materials Interfaces* **2020**, *12* (50), 55649-55658.
19. Biancatelli, R. M. L. C.; Solopov, P. A.; Gregory, B.; Khodour, Y.; Catravas, J. D., HSP90 Inhibitors Modulate SARS-CoV-2 Spike Protein Subunit 1-Induced Human Pulmonary Microvascular Endothelial Activation and Barrier Dysfunction. *J Frontiers in Physiology* **2022**, *13*:812199.
20. Wang, Q.; Zhang, Y.; Wu, L.; Niu, S.; Song, C.; Zhang, Z.; Lu, G.; Qiao, C.; Hu, Y.; Yuen, K. Y.; Wang, Q.; Zhou, H.; Yan, J.; Qi, J., Structural and Functional Basis of SARS-CoV-2 Entry by Using Human ACE2. *Cell* **2020**, *181* (4), 894-904 e9.
21. Shang, J.; Ye, G.; Shi, K.; Wan, Y.; Luo, C.; Aihara, H.; Geng, Q.; Auerbach, A.; Li, F., Structural basis of receptor recognition by SARS-CoV-2. *Nature* **2020**, *581* (7807), 221-224.
22. Lan, J.; Ge, J.; Yu, J.; Shan, S.; Zhou, H.; Fan, S.; Zhang, Q.; Shi, X.; Wang, Q.; Zhang, L.; Wang, X., Structure of the SARS-CoV-2 spike receptor-binding domain bound to the ACE2 receptor. *Nature* **2020**, *581* (7807), 215-220.
23. Daniel Wrapp, N. W., Kizzmekia S. Corbett, Jory A. Goldsmith, Ching-Lin Hsieh, Olubukola Abiona, Barney S. Graham, Jason S. McLellan, Cryo-EM structure of the 2019-nCoV spike in the prefusion conformation. *Science* **2020**, *367*, 1260-1263.
24. Renhong Yan, Y. Z., Yaning Li, Lu Xia, Yingying Guo, Qiang Zhou, Structural basis for the recognition of SARS-CoV-2 by full-length human ACE2. *Science* **2020**, *367*, 1444-1448.
25. Smith, M. C.; Gestwicki, J. E., Features of protein-protein interactions that translate into potent inhibitors: topology, surface area and affinity. *Expert Rev Mol Med* **2012**, *14*, e16.
26. Josephson, K.; Ricardo, A.; Szostak, J. W., mRNA display: from basic principles to macrocycle drug discovery. *Drug Discov Today* **2014**, *19* (4), 388-99.
27. Tai, W.; He, L.; Zhang, X.; Pu, J.; Voronin, D.; Jiang, S.; Zhou, Y.; Du, L., Characterization of the receptor-binding domain (RBD) of 2019 novel coronavirus: implication for development of RBD protein as a viral attachment inhibitor and vaccine. *Cell Mol Immunol* **2020**, *17* (6), 613-620.
28. Zhe Lv, Y.-Q. D., Qing Ye, Lei Cao, Chun-Yun Sun, Changfa Fan, Weijin Huang, Shihui Sun, Yao Sun, Ling Zhu, Qi Chen, Nan Wang, Jianhui Nie, Zhen Cui, Dandan Zhu, Neil Shaw, Xiao-Feng Li, Qianqian Li, Liangzhi Xie, Youchun Wang, Zihe Rao, Cheng-Feng Qin, Xiangxi Wang, Structural basis for neutralization of SARS-CoV-2 and SARS-CoV by a potent therapeutic antibody. *Science* **2020**, *369*, 1505-1509.
29. Sui, J.; Deming, M.; Rockx, B.; Liddington, R. C.; Zhu, Q. K.; Baric, R. S.; Marasco, W. A., Effects of human anti-spike protein receptor binding domain antibodies on severe acute respiratory syndrome coronavirus neutralization escape and fitness. *J Virol* **2014**, *88* (23), 13769-80.
30. Wang, C.; Li, W.; Drabek, D.; Okba, N. M. A.; van Haperen, R.; Osterhaus, A.; van Kuppeveld, F. J. M.; Haagmans, B. L.; Grosveld, F.; Bosch, B. J., A human monoclonal antibody blocking SARS-CoV-2 infection. *Nat Commun* **2020**, *11* (1), 2251.
31. Alina Baum, B. O. F., Elzbieta Wloga, Richard Copin, Kristen E. Pascal, Vincenzo Russo, Stephanie Giordano, Kathryn Lanza, Nicole Negron, Min Ni, Yi Wei, Gurinder S. Atwal, Andrew J. Murphy, Neil Stahl, George D. Yancopoulos, Christos A. Kyratsous, Antibody cocktail to SARS-CoV-2 spike protein prevents rapid mutational escape seen with individual antibodies. *Science* **2020**, *369*, 1014-1018

32. Wibmer, C. K.; Ayres, F.; Hermanus, T.; Madzivhandila, M.; Kgagudi, P.; Oosthuysen, B.; Lambson, B. E.; de Oliveira, T.; Vermeulen, M.; van der Berg, K.; Rossouw, T.; Boswell, M.; Ueckermann, V.; Meiring, S.; von Gottberg, A.; Cohen, C.; Morris, L.; Bhiman, J. N.; Moore, P. L., SARS-CoV-2 501Y.V2 escapes neutralization by South African COVID-19 donor plasma. *Nat Med* **2021**, 27 (4), 622-625.

33. Hamley, I. W., Peptides for Vaccine Development. *ACS Appl Bio Mater* **2022**, 5 (3), 905-944.

34. Benjamin Leader, Q. J. B. a. D. E. G., Protein therapeutics: a summary and pharmacological classification. *Nature reviews / drug discovery* **2008**, 7, 21-39.

35. Rabbani, G.; Ahn, S. N.; Kwon, H.; Ahmad, K.; Choi, I., Penta-peptide ATN-161 based neutralization mechanism of SARS-CoV-2 spike protein. *Biochemistry and Biophysics Reports* **2021**, 28, 101170.

36. Saurabh, S.; Purohit, S. S., A Modified ACE2 peptide mimic to block SARS-CoV2 entry. *bioRxiv* **2020**.

37. Renzi, F.; Gherzi, D., ACE2 fragment as a decoy for novel SARS-CoV-2 virus. *bioRxiv* **2020**, 1-6.

38. Zhang, H.; Penninger, J. M.; Li, Y.; Zhong, N.; Slutsky, A. S., Angiotensin-converting enzyme 2 (ACE2) as a SARS-CoV-2 receptor: molecular mechanisms and potential therapeutic target. *Intensive Care Med* **2020**, 46 (4), 586-590.

39. Monteil, V.; Kwon, H.; Prado, P.; Hagelkruys, A.; Wimmer, R. A.; Stahl, M.; Leopoldi, A.; Garreta, E.; Hurtado Del Pozo, C.; Prosper, F.; Romero, J. P.; Wirnsberger, G.; Zhang, H.; Slutsky, A. S.; Conder, R.; Montserrat, N.; Mirazimi, A.; Penninger, J. M., Inhibition of SARS-CoV-2 Infections in Engineered Human Tissues Using Clinical-Grade Soluble Human ACE2. *Cell* **2020**, 181 (4), 905-913 e7.

40. Rabbani, G.; Ahn, S. N., Roles of human serum albumin in prediction, diagnoses and treatment of COVID-19. *International Journal of Biological Macromolecules* **2021**, 193, 948-955.

41. Cao, B.; Wang, Y.; Wen, D.; Liu, W.; Wang, J.; Fan, G.; Ruan, L.; Song, B.; Cai, Y.; Wei, M.; Li, X.; Xia, J.; Chen, N.; Xiang, J.; Yu, T.; Bai, T.; Xie, X.; Zhang, L.; Li, C.; Yuan, Y.; Chen, H.; Li, H.; Huang, H.; Tu, S.; Gong, F.; Liu, Y.; Wei, Y.; Dong, C.; Zhou, F.; Gu, X.; Xu, J.; Liu, Z.; Zhang, Y.; Li, H.; Shang, L.; Wang, K.; Li, K.; Zhou, X.; Dong, X.; Qu, Z.; Lu, S.; Hu, X.; Ruan, S.; Luo, S.; Wu, J.; Peng, L.; Cheng, F.; Pan, L.; Zou, J.; Jia, C.; Wang, J.; Liu, X.; Wang, S.; Wu, X.; Ge, Q.; He, J.; Zhan, H.; Qiu, F.; Guo, L.; Huang, C.; Jaki, T.; Hayden, F. G.; Horby, P. W.; Zhang, D.; Wang, C., A Trial of Lopinavir-Ritonavir in Adults Hospitalized with Severe Covid-19. *N Engl J Med* **2020**, 382 (19), 1787-1799.

42. Hinman, S. S.; Ruiz, C. J.; Drakakaki, G.; Wilkop, T. E.; Cheng, Q., On-Demand Formation of Supported Lipid Membrane Arrays by Trehalose-Assisted Vesicle Delivery for SPR Imaging. *ACS Appl Mater Interfaces* **2015**, 7 (31), 17122-30.

43. Schneidman-Duhovny, D.; Inbar, Y.; Nussinov, R.; Wolfson, H. J., PatchDock and SymmDock: servers for rigid and symmetric docking. *Nucleic Acids Res* **2005**, 33 (Web Server issue), W363-7.

44. Zhang, G.; Pomplun, S.; Loftis, A. R.; Tan, X.; Loas, A.; Pentelute, B. L., Investigation of ACE2 N-terminal fragments binding to SARS-CoV-2 Spike RBD *bioRxiv* **2020**.

45. Chang, C. C., Recent Advancements in Aptamer-Based Surface Plasmon Resonance Biosensing Strategies. *Biosensors (Basel)* **2021**, 11 (7).

46. Azzouz, A.; Hejji, L.; Kim, K. H.; Kukkar, D.; Souhail, B.; Bhardwaj, N.; Brown, R. J. C.; Zhang, W., Advances in surface plasmon resonance-based biosensor technologies for cancer biomarker detection. *Biosens Bioelectron* **2022**, 197, 113767.

47. Wang, W.; Thiemann, S.; Chen, Q., Utility of SPR technology in biotherapeutic development: Qualification for intended use. *Anal Biochem* **2022**, 654, 114804.

48. Harbour, V.; Casillas, C.; Siddiqui, Z.; Sarkar, B.; Sanyal, S.; Nguyen, P.; Kim, K. K.; Roy, A.; Iglesias-Montoro, P.; Patel, S., Regulation of lipoprotein homeostasis by self-assembling peptides. *ACS Applied Bio Materials*, **2020**, 3 (12), 8978-8988.

49. Schuck, P.; Zhao, H., The role of mass transport limitation and surface heterogeneity in the biophysical characterization of macromolecular binding processes by SPR biosensing. *Methods Mol Biol* **2010**, 627, 15-54.
50. Larue, R. C.; Xing, E.; Kenney, A. D.; Zhang, Y.; Tuazon, J. A.; Li, J.; Yount, J. S.; Li, P. K.; Sharma, A., Rationally Designed ACE2-Derived Peptides Inhibit SARS-CoV-2. *Bioconjug Chem* **2021**, 32 (1), 215-223.
51. Yang, J.; Petitjean, S. J. L.; Koehler, M.; Zhang, Q.; Dumitru, A. C.; Chen, W.; Derclaye, S.; Vincent, S. P.; Soumillion, P.; Alsteens, D., Molecular interaction and inhibition of SARS-CoV-2 binding to the ACE2 receptor. *Nat Commun* **2020**, 11 (1), 4541.
52. Bruno, B. J.; Miller, G. D.; Lim, C. S., Basics and recent advances in peptide and protein drug delivery. *Ther Deliv* **2013**, 4 (11), 1443-67.

Graphic Content

